# Whole-brain deactivations precede uninduced mind-blanking reports

Abbreviated title: Mind-blanking and whole-brain deactivations

Paradeisios Alexandros Boulakis[1,2], Sepehr Mortaheb[1,2], Laurens van Calster[2,3,4,5], Steve Majerus[2,3,4], Athena Demertzi[1,2,3,*]

[1]Physiology of Cognition Lab, GIGA-Cyclotron Research Center In Vivo Imaging, Allée du 6 Août 8 (B30), 4000, University of Liège Liège, Belgium

[2]Fund for Scientific Research FNRS, Rue d'Egmont 5, B – 1000, Brussels, Belgium

[3]Psychology and Neuroscience of Cognition Research Unit, Place des Orateurs 3 (B33), 4000, University of Liège Liège, Belgium

[4]GIGA-Cyclotron Research Center In Vivo Imaging, Allée du 6 Août 8 (B30), 4000, University of Liège Liège, Belgium

[5]Department of Neurology, Cliniques universitaires Saint-Luc, Av. Hippocrate 10, 1200 Brussels, Belgium

* Corresponding author mail: `a.demertzi@uliege.be`

Page Count: 29

Figure Count: 4

Table Count: 3

Abstract Word Count: 232

Introduction Word Count: 642

Discussion Word Count: 1466

Disclosure of competing interests: The authors declare no competing interests.

## Abstract

Mind-blanking (MB) is termed as the experience of inability to report mental contents. In contrast to other mental states, such as mind-wandering or sensory perceptions, the neural correlates of MB started getting elucidated only recently. A notable particularity that pertains to MB studies is the way MB is instructed for reports, like by deliberately asking participants to "empty their minds". Such instructions were shown to induce fMRI activations in frontal brain regions, typically associated with metacognition and self-evaluative processes, suggesting that MB may be a result of intentional mental content suppression. Here, we aim at examining this hypothesis by determining the neural correlates of MB without induction. Using fMRI combined with experience-sampling, univariate analysis of MB reports revealed deactivations in occipital, frontal, somatosensory, and thalamic areas, but no activations in prefrontal regions. In fact, a Bayesian region-of-interest analysis on areas previously shown to be implicated in MB provided evidence for frontal deactivations during MB reports in comparison to other mental states. Further contrast analysis between reports of MB and content-oriented mental states also revealed deactivations in the L angular gyrus. We propose that these effects characterize a cortical profile of MB, where key cortical nodes are unable to communicate and formulate reportable content. Collectively, our results show that study instructions for MB may lead to cortical differences which provide different insights as to the underlying mechanisms leading to the phenomenology of MB.



Keywords: mind-blanking, fMRI experience-sampling, spontaneous thinking, mental content, angular gyrus, anterior cingulate cortex

## Significance Statement

An emergent research paradigm in the study of mental states has focused on periods of complete thought absence, where people report an inability to report mental content, termed mind blanking. The neural correlates supporting mind blanking are still debated and might vary depending on thought-report instructions. By reanalyzing an fMRI dataset utilizing an unguided, free-thinking paradigm, the present study provides critical insights into the neuronal events that preceded mind-blanking reports. Our findings demonstrate that spontaneous mind-blanking occurrences are associated with large-scale cortical deactivations in frontal, occipital, parietal and thalamical sites, with the frontal evaluative sites and the angular gyrus especially differentiating mind-blanking from other mental states associated with the presence of content.

# Introduction

During spontaneous thinking, mental content appears continuous and seamless (Christoff et al., 2009). Probing people to report what they think yields a variety of mental states with distinct contents and attitudes towards those contents, such as daydreaming, task engagement, and mind wandering (Van Calster et al., 2017; Smallwood et al., 2021). A critical component of these states is the presence of content. Sporadically, however, people will experience the inability to report their immediate mental state. This phenomenological experience of no thought is termed as mind-blanking (MB; (Ward and Wegner, 2013).

Recent research into the neural correlates of MB using fMRI experience-sampling (i.e., asking people at random times to report their immediate mental state, (Smallwood and Schooler, 2015; Weinstein, 2018) showed that spontaneous MB reports were close to a cerebral configuration characterized by a positive all-to-all connectivity profile (Mortaheb et al., 2022). Such pattern of overall positive statistical dependencies implies that all cortical regions communicate in the same way when MB is reported. It is of interest that similar functional organization is observed in NREM sleep (El-Baba et al., 2019), suggesting that MB might be the result of overall low cortical arousal. Similar evidence was found on shorter timescales using EEG, where localized slow-wave activity was linked with MB reports, leading to the possibility of cerebral "local sleeps" during MB (Andrillon et al., 2019). Indeed, posterior electrode slow-wave activity during a go/no-go task was predictive of MB reports, in contrast to frontal electrode slow-waves which were linked to mind-wandering (Andrillon et al., 2021). Collectively, these studies propose that MB events are tied to neuronal profiles which do not permit efficient cortical communication, therefore hindering people from reporting clear mental content (Mortaheb et al., 2022).

A notable particularity of MB studies is the way MB is instructed for report. For example, Kawagoe et al. (2019) studied MB by asking people to actively "empty their minds" until they experience no thoughts, upon when they reported they had achieved this state. By analyzing the fMRI BOLD signal preceding these reports, the authors found deactivations in Broca's area and the left hippocampus, and activations in the ventromedial prefrontal cortex (vmPFC)/ subgenual region of the anterior cingulate cortex (subACC). The authors interpreted these results as reduced inner speech, elicited by the attempt of the participants to silence

internally-generated thoughts. This possibility was considered before, primarily in the context of mind wandering. As our thoughts spontaneously transition across an internal-external milieu (Vanhaudenhuyse et al., 2011; Smallwood et al., 2012; Demertzi et al., 2015), the ACC serves executive functions, such as identifying attentional lapses from ongoing tasks (Christoff et al., 2009) or allowing thought transitions to be controlled (Crespo-García et al., 2022). In similar lines, self-induced MB also requires constant supervision of thoughts in the form of evaluating ongoing experience in order to promote thought-silencing, therefore recruiting regions such as the vmPFC/subACC, a central hub for mental state evaluative processes (Jenkins and Mitchell, 2011; Qin et al., 2020). Evidence for this possibility comes from a case study of an experienced meditator (meditating > 12 h/day for 10 years, estimated total > 50,000 hours), which showed decreases in fMRI connectivity between the posterior cingulate cortex and mesio-frontal regions when he was practicing content-free vs. content-related meditation (Winter et al., 2020). Taken together, the use of MB induction in neuroimaging studies might provide a biased picture about the underlying neural mechanisms of MB, as the MB induction paradigm may reflect the neural substrates of the command to "empty the mind" rather than MB per se.

By means of fMRI combined with experience-sampling we here performed univariate analysis to test whether MB reports would recruit vmPFC-subACC activations also in free-thinking (no induction) conditions, examining the hypothesis that during MB, we will observe disengagement of frontal sites, as MB represents a failure to bring content into our awareness.

# Materials and Methods

## Experience-Sampling Dataset / Experimental Design

We used previously collected data (Van Calster et al., 2017) acquired during resting-state with eyes open in a 3T head-only scanner (Magnetom Allegra, Siemens Medical Solutions, Erlangen, Germany). At random intervals ranging from 30 to 60 seconds, participants were probed with an auditory cue to report via button press what was in their mind at the moment just preceding the cue. Each probe started with the appearance of an exclamation mark lasting for 1000 ms inviting the participants to review and characterize the cognitive event(s) they just experienced. After this period, participants were presented with 4 options, classifying their mental content as: a) Absence, defined as MB or empty state of mind, b) Perceptions, defined as thought-free

attentiveness to stimuli via the senses, and c) Thoughts (Figure 1). In the case of a "Thought" report, participants were asked to report if the content was stimulus-dependent (sDEP; thoughts evoked from the immediate environment) or stimulus-independent (sIND; thoughts irrelevant from the immediate environment). Depending on the probes' trigger times and participants' reaction times, the duration of the recording session was variable (48-58 min). To minimize misclassification rates, participants had a training session outside of the scanner at least 24 hours before the actual session.

The dataset contains structural and functional MRI volumes for 36 healthy, right-handed participants (27 female, mean = 23, std = 3, range = [18,30]). Five participants were excluded as they did not report each mental state option at least once (total participants = 31). All participants gave their written informed consent to take part in the experiment. The study was approved by the ethics committee of the University Hospital of Liège.

## fMRI acquisition parameters

fMRI data were acquired with standard transmit–receive quadrature head coil using a T2*-weighted gradient-echo EPI sequence with the following parameters: repetition time (TR) = 2040 msec, echo time (TE) = 30 msec, field of view (FOV) = 192×192 mm2, 64×64 matrix, 34 axial slices with 3 mm thickness and 25% interslice gap to cover most of the brain. A high-resolution T1-weighted MP-RAGE image was acquired for anatomical reference (TR = 1960 msec, TE = 4.4 msec, inversion time = 1100 msec, FOV = 230×173 mm, matrix size = 256×192×176, voxel size = 0.9×0.9×0.9 mm). The participant's head was restrained using a vacuum cushion to minimize head movement. Stimuli were displayed on a screen positioned at the rear of the scanner, which the participant could comfortably see using a head coil-mounted mirror.

## Statistical Analysis

**Preprocessing**. Structural and functional images were preprocessed using a locally developed pipeline written in the Nipype module (v1.8.2; https://nipype.readthedocs.io/) in Python (v3.8), combining functions from Statistical Parametric Mapping software (SPM12; `https://www.fil.ion.ucl.ac.uk/spm/`), the FMRIB Software Library v6.0 (FSL; `https://fsl.fmrib.ox.ac.uk/fsl/fslwiki`) and the Artifact Detections Tools (ART; `https://www.nitrc.`

org/projects/artifact_detect). For each node of the pipeline, we have specified the respective module and function used. Structural images were skull stripped (fsl.Bet), bias-field corrected, and segmented into white matter, grey matter, and cerebrospinal fluid (spm.Segment). Finally, the restored, bias-corrected structural image was normalized into the standard stereotaxic Montreal Neurological Institute (MNI) space (spm.Normalize). The first volume of the functional data was removed to avoid T1 saturation effects (fsl.ExtractROI). Then, the scans were realigned to the mean functional volume (spm.Realign) using a 2nd B-spline interpolation with least-squares alignment. We used the realignment parameters to estimate motion outlier scans. An image was defined as an outlier or artifact image if the head displacement in the x, y, or z direction was greater than 3 mm from the previous frame, if the rotational displacement was greater than 0.05 rad from the previous frame, or if the global mean intensity in the image was greater than 3 SDs from the mean image intensity for the entire scans. The realignment parameters were also saved to a file so that these variables can be used as regressors when modeling subject-level BOLD activity. The realigned were slice-scan time corrected to account for the accumulation of offset delays between the first slice and the remaining slices (fsl.SliceTimer). Then, the images were coregistered to the participant space using the bias-corrected structural image as the target and a normalized mutual information function (spm.Coregister) and then normalized to MNI space (spm.Normalize). Finally, the normalized images were smoothed using a Gaussian kernel of 8-mm full width at half-maximum.

**Univariate whole-brain analysis**. Data were analyzed using a univariate linear general linear model (GLM). The 4 responses of the participants (Absence, Perception, Stimulus Independent Thought and Stimulus Dependent Thought) were modeled and convolved with the canonical hemodynamic response function (HRF) as regressors of interest for each participant in the first-level analysis. Each response instance was modeled as an epoch starting 5 TRs before probe onset, following evidence from a "thinking aloud" paradigm that showed that mental states tend to fluctuate slowly, with one experience being reported every 10s (Van Calster et al., 2017). With the aim to comprehensively account for the hemodynamic response function, supplementary analyses were performed with 7TR and 2TR before the probe. Each participant's six motion parameters (three rigid body translations and three rotations from the realignment procedure) were included to regress out effects related to head movement-related

variability. We used a high-pass filter cutoff of 1/128 Hz to remove the slow signal drifts with a longer period, and a first-order autoregressive model (AR (1)) was used for serial correlations with the classical restricted maximum likelihood (REML) parameter. Regionally specific condition effects were tested using linear contrasts for each key event relative to the baseline and each participant. Contrasts for "Perception" and "Thinking" regressors have been reported elsewhere (Van Calster et al., 2017). Therefore, here we tested for contrasts specific to MB. Given 4 regressors: [MB, Perception, sDEP, sIND], subject-level analysis yielded the following T contrasts of interest: a) Positive Effects of MB [1 0 0 0], b) Negative Effects of MB [-1 0 0 0], c) MB > Thinking [2 0 -1 -1], d) Thinking > MB [-2 0 1 1], e) MB > Perception [1 -1 0 0], f) Perception > MB [-1 1 0 0], g) Absence > Content [3 -1 -1 -1], h) Content > Absence [-3 1 1 1]. The resulting contrast parameter estimates from the individual subject-level were entered into a random effects model for a second level analysis, using a one-sided, one-sample T-test. All maps were thresholded at a whole-brain $p_{uncorrected}$ <.001 and FDR-corrected at cluster-level $p < .05$. In case the resulting maps yielding no voxels and given the sparseness of MB reports across participants, for exploratory purposes we also examined the maps using a $p_{uncorrected}$ <.001 and a cluster threshold of 50 adjacent voxels.

**Region of interest (ROI) analysis**. . Based on the a-priori hypothesis about the role of the ACC in monitoring thought contents, we additionally performed a ROI analysis based on MNI coordinates reported in Kawagoe et al. (2019) for the ACC (MNI: 3,39,-5). To examine whether previous findings on the neuronal correlates of MB during active mental silencing can be extended to spontaneous blanking periods in ongoing mentation, we also included the left hippocampus (MNI: -27,-33,-3) and Broca's area (MNI: -47,26,20).To extract single-participant beta parameters for each regressor of interest, 5-mm radius binary spheres were created for each ROI using the flsmaths function of the FSL software, which were then used to mask first-level subject-specific beta parameter maps, and extract the signal of interest. Localization of the ROIs was performed based on the MNI coordinates reported in Kawagoe et al. (2019) (See Supplementary Figure 1).

Given our hypothesis for the absence of frontal engagement in MB and the reduced statistical power of traditional frequentist approaches due to multiple comparisons, we opted for Bayesian Linear Modelling (McElreath, 2020), allowing us to make inferences on potential null results

while not being overly conservative. For each ROI, we fit a linear model with beta values as a dependent variable, allowing the intercept to freely vary as a function of mental state.

$$Beta \sim \ a[mentalstate] + error$$

As prior for the intercept, we chose a normal distribution as it is the maximum entropy distribution (or "least surprising") for any random variable with an unknown mean and unknown, finite variance. Effectively, a maximum entropy distribution is the most probable distribution for a random variable, given the potential constraints placed on its parameters. We chose to model the intercepts as $N(0, 1)$, as we expected small effects. To examine the robustness of our choice of priors, we constructed two variants of normal distributions, one skeptical distribution that reduces effect sizes close to 0 by having high precision, marked as low variance $N(0, .5)$, and one lax prior, marked by low precision, permitting extreme effects $N(0, 3)$. Prior predicative simulation for the skeptical prior places the mass of effect sizes of each state within half a standard deviation from the mean. Likewise, the lax prior places the mass of effect sizes within 3 standard deviations. Additionally, we also fit a model using a uniform prior $U(-2, 2)$, giving equal probability to effect sizes within two standard deviations from the mean. To further validate that our priors generated the desired ranges of parameters, we sampled from the prior distribution to perform a prior predictive visual check.

We estimated one posterior distribution for each one of the intercepts of the 4 mental states. Difference posterior was estimated by the pairwise subtraction of the mental state intercepts. Posterior distributions are summarized by their median, their standard deviation, and the 95% highest density intervals (HDI), representing the 95% probability that the true parameter lies within that range. To validate that the posterior accurately represented a generative model of the data, we also performed posterior predictive simulations, to examine if the ranges of our model can encompass the different beta values.

To fit the models, we used a Markov Chain Monte-Carlo No U-Turn Sampler (MCMC-NUTS). MCMC is a class of algorithms for sampling from an unknown posterior distribution. The sampler uses a stochastic, random-walk procedure to draw samples from a random variable, and then approximates the desired distribution by integrating across the sum of the drawn samples (Harrison, 2010). The NUTS sampler is the mechanism of effective sample generation.

As MCMC is sensitive to its tuning parameters, NUTS facilitates the sampling process by providing good candidate points in the distribution for the algorithm to sample (Hoffman and Gelman, 2011). To examine the convergence of the models, we sampled the posterior from 4 different chains, and both visually inspected the traceplot for points in the sampling procedure where the sampler stuck and accepted a model only if its scale reduction factor was at 1.00. The stability of estimates was evaluated using an effect sample size (ESS) $> 10000$. We sampled 5000 samples from the posterior, with 2000 samples as burn-in.

Each model was compared to a null model:

$$Beta\ a + error$$

where the intercept does not differentiate between the mental states, effectively representing the mean of the mental states. Model fitting was performed using the PYMC3 (`https://docs.pymc.io/en/v3/index.html`) Python package Salvatier et al. (2016).

# Results

**fMRI univariate analysis reveals whole-brain deactivations.**. Initially, we focused on identifying regions associated with spontaneous MB occurrence during ongoing mentation. Overall, we found deactivation in the anterior /midcingulate cortex, the calcarine cortex, the bilateral thalami, the right anterior insula, the precentral gyrus, and the left superior parietal lobule (Figure 2, Table 1). To validate these results, we also examined different TRs around the probe period. Although an uncorrected voxel-level threshold of $p = 0.01$ recurrently showed deactivation in frontal, parietal and thalamical regions, cluster correction showed that only the thalamus was consistently deactivated across all time increments (See Supplementary Figures 2-3).

At the FDR cluster threshold ($p<.05$), the contrast between MB and the other mental states did not identify significant number of voxels. When the threshold was lowered to the exploratory level of whole-brain $p<.001$, voxels$> 50$, deactivations were observed in the angular gyrus (n voxels: 70, Z = 3.78, x = -60, y = -58, z = 32), a finding mainly driven by consistent deactivation of MB reports compared to stimulus dependent and stimulus independent thoughts (Figure 3).

**fMRI Bayesian ROI analysis provides evidence of deactivations in the vmPFC / subACC**. Based on our a-priori assumptions on the role of vmPFC / subACC in thought monitoring, we wanted to examine the clusters reported in Kawagoe et. al, 2019. We specified 5mm regions of interest in the vmPFC/subACC, Broca's area and the left hippocampus, and extracted the mean timeseries of the signal 5 TR preceding mental state reports. Then for each ROI, we run a Bayesian contrast analysis using physiologically plausible priors about the behavior of beta parameters across the four reported mental states (See Methods for the justification of priors) (Figure 4-A,4-B). Extensive descriptive statistics of the posterior distributions for each ROI and mental state are presented in Table 2. Overall, the only intercept that did not include 0 in its 95% credibility intervals was MB in the vmPFC/subACC (Median: -0.235, SD: 0.117, HDI (0.025): -0.467, HDI (0.975): -0.009), providing evidence of important deactivations in the vmPFC/subACC (4-C). The other states did not show any significance for evidence in either direction (Supplementary Figure 4-5). We further tested pairwise comparisons of MB beta parameters with each other mental state, as well as a contrast analysis of MB with the other 3 mental states. To examine pairwise comparison, we decided to do inference of the posteriors by subtracting the MB posterior of each ROI with the posterior of the rest of the mental states. Extensive results of the posterior of the differences are presented in Table 2 (Supplementary Tables 1,3,5 for the rest of the examined priors). We only found evidence for the vmPFC/subACC, namely MB reports were associated with reliably lower beta values that the other three mental states (Median: -0.300, SD: 0.119, HDI (0.025): -0.539, HDI (0.975): -0.066), as well as in the contrast MB-SInd (Median: -0.367, SD: 0.168, HDI (0.025): -0.690, HDI (0.975): -0.028) (Figure 4). These results were replicated with the other examined priors (Supplementary Figures 6-14). To further validate whether the fitted models performed better against null models with only one intercept, for each fitted ROI model we estimated the Watanabe-Akaike information criterion (WAIC) of the fitted and null model, as well as the expected log pointwise predictive density using leave-one-out cross-validation. Only for betas in the ACC did the model containing multiple intercepts perform better than the null model ($\text{Fitted}_{\text{WAIC}}$ -130.438 $<$ $\text{Null}_{\text{WAIC}}$ : -130.790 , $\text{Fitted}_{\text{ELPD}}$ : -130.653 $<$ $\text{Null}_{\text{ELPD}}$ : -130.891) (Table 3). This was replicated for the rest of the chosen priors (Supplementary Tables 2,4,6).

## Discussion

We re-analyzed an experience-sampling dataset paired with fMRI to examine the neural correlates of MB in typical individuals during unconstrained mentation with the aim to delineate how instructions influence MB's neural correlates. Our results suggest that spontaneous un-induced MB is supported by deactivations of thalamo-cortical regions as compared to mental states with reportable content, which go in a different direction from what has been reported so far.

We first show that whole-brain thalamo-cortical deactivations precede MB reports. Specifically, the fMRI univariate analysis highlighted a cluster of regions comprising the anterior / midcingulate cortex, the calcarine cortex, the bilateral thalami, the right anterior insula, the precentral gyrus, and the left superior parietal lobule that systematically deactivated when people reported MB. Cortical deactivations have been associated with reduced neuronal resource allocation (Hester et al., 2004) and impaired cognitive performance (Ji et al., 2010). Hairston et al. (2008) found that cross-modal deactivations in occipital, frontal and parietal cortices correlated with difficulty in an auditory task, providing further evidence for the significance of deactivations in neuronal resource allocation. Overall, we think that the here identified whole-brain deactivations represent as brief periods of disengagement, during which the brain cannot support attentional and mental-reporting processes.

This idea is further supported by the finding that two key subclusters we deactivated: the primary visual cortex and multiple cortical nodes of the salience network (Seeley et al., 2007). Previous work has suggested that thoughts unrelated to the immediate environment involve the decoupling of sensory areas from regions contributing to stimulus salience (Mittner et al., 2016). Here, we propose that deactivations in the calcarine areas and the salience network nodes might reflect decreased sensitivity to environmental cues. Indeed, instructing participants to think of nothing results in deactivation between the DMN and the sensory cortices, potentially reflecting this decoupling of the sensory system and a system of internal thoughts (Kawagoe et al., 2018). The whole-brain disengagement explanation is also supported by the deactivation of the thalamus, a recurrent node in saliency and engagement in mental state reportability (Kucyi et al., 2013; Philippi et al., 2021). Thalamic activity covaries with attentional demands, such that increased executive control (Jansma et al., 2000; Dosenbach

et al., 2008) and selective attention (Raeva, 2006; Antonucci et al., 2021) have been linked to increased thalamic involvement. Potentially, the integrative nature of the thalamus (Hwang et al., 2017) is necessary to cast a mental spotlight and selectively allocate resources to bring a specific thought into conscious awareness. Overall, the rich profile of deactivations preceding MB reports highlights the important role of cortical nodes, traditionally associated with the salience of information and monitoring of ongoing cognition.

Examining report-specific effects, we also found that MB, compared to the other content-oriented mental states was characterized by deactivation in the left angular gyrus. Part of the parietal association cortex (Seghier, 2013), the angular gyrus has been associated with a range of cognitive functions such as semantic processing (Binder et al., 2009; Kuhnke et al., 2022), internal mentation (Ramanan et al., 2018), attentional orientation (Cattaneo et al., 2009) and volitional mnemonic processing (i.e;, top-down recall ; (Ciaramelli et al., 2008; Ciaramelli and Moscovitch, 2020). Additionally, when participants let their minds wander, one of the core regions systematically activated when reporting content-full spontaneous thoughts is the angular gyrus (Christoff et al., 2004; Fox et al., 2005; Sormaz et al., 2018), irrespective of age (Maillet et al., 2019) or past/future orientation (Ramanan et al., 2018). Our results supplement these findings by showing that deactivations in the angular gyrus are associated with an inability to report mental content at any level of detail. Our results also are in line with previous electrophysiological results, where MB attentional lapses during task engagement were predicted by posterior transient slow-wave activity in the form of delta-band waves (Andrillon et al., 2021). The authors emphasized the role of parietal cortices in the emergence of conscious reports, where slow wave activity might inhibit parietal-frontal communication and lead to the MB experience. We supplement this explanation by proving more granular structural information, introducing the angular gyrus as a key parietal node.

The ROI analysis shows the specificity of a deactivated ACC/vmPFC in MB, a cluster previously reported as activated during MB. Frontal contributions during thought-monitoring tasks are typically associated with meta-cognition functions, where participants monitor the content of their conscious awareness, for which the ACC appears implicated (Chin and Schooler, 2009). Additional ACC activations were observed during mind-wandering with no meta-awareness as compared to periods of mind-wandering with awareness (Christoff et al., 2009). The au-

thors interpreted these larger activations as the ACC signaling a mismatch between expected thought stream and actual, wandering thoughts, eliciting a higher degree of surprise to the participant (Christoff et al., 2009). However, given the multiple partitions of the ACC, treating it as a unimodal region that collectively contributes to one specific cognitive process might be misleading in the context of mental state evaluation. In our study, the cluster originated close to the borders between ACC and vmPFC, denoting that previous effects reported might additionally signal processes. Indeed, the vmPFC-ACC cluster is systematically implicated in evaluative (Jenkins and Mitchell, 2011; D'Argembeau, 2013)(for a list of studies associated with this specific cluster, please see `https://neurosynth.org/locations/?x=4&y=40&z=-4`) and metacognitive processes Vaccaro and Fleming (2018), which are facilitatory to the internal stream of thought (Smallwood et al., 2012; Vincent et al., 2008). Given the metacognitive aspect of ACC-vmPFC, we here interpret these deactivations as failures to recurrently examine the content of a thought, which can be formulated as self-referential questions ("Am I thinking of anything?") (D'Argembeau et al., 2007).

To our knowledge, only one study has examined the fMRI neural correlates of MB from a univariate perspective before (Kawagoe et al., 2019). In that protocol, when participants were instructed to "think of nothing", there were deactivations in the Broca's area and the left hippocampus, and activations in the subgenual parts of the anterior cingulate cortex (ACC). Similar frontal activations have been observed in clinical settings, where patients with depressive symptoms were guided to suppress their thoughts, in order to prevent rumination (Wyland et al., 2003; Carew et al., 2015). By bridging the current literature together, we suggest that the discrepancy between spontaneous and self-induced MB may reflect not only differences in methodologies, but also might point to the existence of different forms of MB, as well. As has been the case for mind-wandering, for which intentional and unintentional forms have been proposed (Seli et al., 2016), different mind-wandering forms might be differentiated by the distinct involvement of higher-order frontal regions associated with cognitive control. In similar lines, we propose the possibility of intentional MB, originating from top-down monitoring of keep thoughts out of our mental events, such as during meditative practices, and unintentional MB that originates from spontaneous lapses of frontal-sensory-thalamic systems that monitor the stream of consciousness and an inability to attribute semantic content to our mental life.

While this interpretation is still speculative and the clear presence of different MB forms cannot be extrapolated from our dataset, it paves a promising avenue for future research contrasting different forms of thought "absence".

Our study leaves several questions unanswered. As with most fMRI experience-sampling studies, the duration of mental states is dependent on the specified sampling rate, meaning that low-frequency states such as MB might be under-sampled. Akin to this problem, the sampling rate might not be fast enough to sample states that might be transient, such as MB (Mortaheb et al., 2022). Therefore, current paradigms should be complemented with faster neuroimaging sampling methods, such as EEG, which permit estimation of brain dynamics at the sub-second level, and potentially can uncover momentary markers of MB. Additionally, the analyses of the present study might be sensitive to the assumed period that a mental state lasts: we assumed a uniform 10s period for all mental states. However, future research should develop paradigms that consider the variable duration of specific mental states, based on unsupervised multivariate neural pattern decoding techniques. A final limitation originates from the nature of our analysis. In our previous work (Mortaheb et al., 2022), we showed that the amplitude of the global signal, a correlate of cortical and physiological arousal, can predict MB occurrences. While univariate regression provides correlative evidence for the neural correlates of MB, it does not provide a physiological account of how deactivations might originate.

To summarize, we examined the neural correlates of uninduced MB under free-thinking conditions. Our results point to unique thalamocortical contributions in thought reportability, and potential presence of multiple avenues of thought absence. As the topic of absence of thoughts has wide experimental, philosophical, and potentially clinical implications about the understanding of the thought-oriented and stimulus-driven mind, we believe further research can incorporate mind blanks in the study of the stream of consciousness.

## Author Contributions

**Paradeisios Alexandros Boulakis**: Conceptualization, Methodology, Software, Formal analysis, Data Curation, Writing - Original Draft, Visualization, Validation, Funding acquisition.**Sepehr Mortaheb**: Methodology, Data Curation, Writing - Review & Editing, Software. **Laurens van Calster**: Resources, Data Curation, Writing - Review & Editing. **Steve Ma-**

**jerus**: Resources, Methodology, Data Curation, Writing - Review & Editing. textbfAthena Demertzi: Conceptualization, Methodology, Writing - Original Draft, Supervision, Funding acquisition.

## Funding Sources

This article was supported by the Belgian Fund for Scientific Research (FRS-FNRS), the Léon Fredericq Foundation, and the University and of University Hospital of Liège. It was also based upon work from COST Action CA18106, supported by COST (European Cooperation in Science and Technology.

## Code Accesibility

All codes to replicate the analysis is available on `https://gitlab.uliege.be/Paradeisios.Boulakis/mb_activation` (Boulakis, 2023). The code is based on existing Python libraries and custom functions. The provided repository contains all the necessary information to install an environment and reproduce the analysis on the experience-sampling dataset. We used an existing experience-sampling dataset, during which participants had the option to report the absence of thoughts (Van Calster et al., 2017). Previous research on this dataset, examining has replicated consistent fMRI findings in other mental states (MW: DMN and executive cortical areas). The raw data are also freely available in BIDS format from: `https://openneuro.org/datasets/ds004134/versions/1.0.0`.

# References


Andrillon T, Burns A, Mackay T, Windt J, Tsuchiya N (2021) Predicting lapses of attention with sleep-like slow waves. Nat Commun 12:3657.

Andrillon T, Windt J, Silk T, Drummond SPA, Bellgrove MA, Tsuchiya N (2019) Does the Mind Wander When the Brain Takes a Break? Local Sleep in Wakefulness, Attentional Lapses and Mind-Wandering. Front Neurosci 13:949.

Antonucci LA, Penzel N, Pigoni A, Dominke C, Kambeitz J, Pergola G (2021) Flexible and specific contributions of thalamic subdivisions to human cognition. Neurosci Biobehav Rev 124:35–53.

Binder JR, Desai RH, Graves WW, Conant LL (2009) Where Is the Semantic System? A Critical Review and Meta-Analysis of 120 Functional Neuroimaging Studies. Cereb Cortex 19:2767–2796.

Boulakis PA (2023) Mind_Blanking_Deactivations_Codes.

Carew CL, Tatham EL, Milne AM, MacQueen GM, Hall GB (2015) Design and Implementation of an fMRI Study Examining Thought Suppression in Young Women with, and At-risk, for Depression. J Vis Exp p. 52061.

Cattaneo Z, Silvanto J, Pascual-Leone A, Battelli L (2009) The role of the angular gyrus in the modulation of visuospatial attention by the mental number line. Neuroimage 44:563–568.

Chin JM, Schooler JW (2009) Meta-Awareness In Banks WP, editor, Encyclopedia of Consciousness, pp. 33–41. Academic Press, Oxford.

Christoff K, Gordon AM, Smallwood J, Smith R, Schooler JW (2009) Experience sampling during fMRI reveals default network and executive system contributions to mind wandering. Proc Natl Acad Sci U S A 106:8719–8724.

Christoff K, Ream JM, Gabrieli JDE (2004) Neural Basis of Spontaneous thought Processes. Cortex 40:623–630.

Ciaramelli E, Grady CL, Moscovitch M (2008) Top-down and bottom-up attention to memory: A hypothesis (AtoM) on the role of the posterior parietal cortex in memory retrieval. Neuropsychologia 46:1828–1851.

Ciaramelli E, Moscovitch M (2020) The space for memory in posterior parietal cortex: Reanalyses of bottom-up attention data. Neuropsychologia 146:107551.

Crespo-García M, Wang Y, Jiang M, Anderson MC, Lei X (2022) Anterior Cingulate Cortex Signals the Need to Control Intrusive Thoughts during Motivated Forgetting. J Neurosci 42:4342–4359.

D'Argembeau A (2013) On the Role of the Ventromedial Prefrontal Cortex in Self-Processing: The Valuation Hypothesis. Front Hum Neurosci 7.

D'Argembeau A, Ruby P, Collette F, Degueldre C, Balteau E, Luxen A, Maquet P, Salmon E (2007) Distinct regions of the medial prefrontal cortex are associated with self-referential processing and perspective taking. J Cogn Neurosci 19:935–944.

Demertzi A, Antonopoulos G, Heine L, Voss HU, Crone JS, de Los Angeles C, Bahri MA, Di Perri C, Vanhaudenhuyse A, Charland-Verville V, Kronbichler M, Trinka E, Phillips C, Gomez F, Tshibanda L, Soddu A, Schiff ND, Whitfield-Gabrieli S, Laureys S (2015) Intrinsic functional connectivity differentiates minimally conscious from unresponsive patients. Brain 138:2619–2631.

Dosenbach NU, Fair DA, Cohen AL, Schlaggar BL, Petersen SE (2008) A dual-networks architecture of top-down control. Trends Cogn Sci 12:99–105.

El-Baba M, Lewis DJ, Fang Z, Owen AM, Fogel SM, Morton JB (2019) Functional connectivity dynamics slow with descent from wakefulness to sleep. PLOS ONE 14:e0224669.

Fox MD, Snyder AZ, Vincent JL, Corbetta M, Van Essen DC, Raichle ME (2005) The human brain is intrinsically organized into dynamic, anticorrelated functional networks. Proc Natl Acad Sci U S A 102:9673–9678.

Hairston WD, Hodges DA, Casanova R, Hayasaka S, Kraft R, Maldjian JA, Burdette JH (2008)

Closing the mind's eye: Deactivation of visual cortex related to auditory task difficulty. NeuroReport 19:151.

Harrison RL (2010) Introduction To Monte Carlo Simulation. AIP Conf Proc 1204:17–21.

Hester RL, Murphy K, Foxe JJ, Foxe DM, Javitt DC, Garavan H (2004) Predicting Success: Patterns of Cortical Activation and Deactivation Prior to Response Inhibition. J Cogn Neurosci 16:776–785.

Hoffman MD, Gelman A (2011) The No-U-Turn Sampler: Adaptively Setting Path Lengths in Hamiltonian Monte Carlo. arXiv 1111.4246. https://doi.org/10.48550/arXiv.1111.4246.

Hwang K, Bertolero MA, Liu WB, D'Esposito M (2017) The Human Thalamus Is an Integrative Hub for Functional Brain Networks. J Neurosci 37:5594–5607.

Jansma JM, Ramsey NF, Coppola R, Kahn RS (2000) Specific versus nonspecific brain activity in a parametric N-back task. Neuroimage 12:688–697.

Jenkins AC, Mitchell JP (2011) Medial prefrontal cortex subserves diverse forms of self-reflection. Soc Neurosci 6:211–218.

Ji G, Sun H, Fu Y, Li Z, Pais-Vieira M, Galhardo V, Neugebauer V (2010) Cognitive Impairment in Pain through Amygdala-Driven Prefrontal Cortical Deactivation. J Neurosci 30:5451–5464.

Kawagoe T, Onoda K, Yamaguchi S (2018) Different pre-scanning instructions induce distinct psychological and resting brain states during functional magnetic resonance imaging. Eur J Neurosci 47:77–82.

Kawagoe T, Onoda K, Yamaguchi S (2019) The neural correlates of "mind blanking": When the mind goes away. Hum Brain Mapp 40:4934–4940.

Kucyi A, Salomons TV, Davis KD (2013) Mind wandering away from pain dynamically engages antinociceptive and default mode brain networks. Proc Natl Acad Sci U S A 110:18692–18697.

Kuhnke P, Chapman CA, Cheung VKM, Turker S, Graessner A, Martin S, Williams KA, Hartwigsen G (2022) The role of the angular gyrus in semantic cognition: A synthesis of five functional neuroimaging studies. Brain Struct Funct .

Maillet D, Beaty RE, Adnan A, Fox KCR, Turner GR, Spreng RN (2019) Aging and the wandering brain: Age-related differences in the neural correlates of stimulus-independent thoughts. PLoS One 14:e0223981.

McElreath R (2020) Statistical Rethinking: A Bayesian Course with Examples in R and STAN. Chapman and Hall/CRC, New York,USA, New York,USA, second edition.

Mittner M, Hawkins GE, Boekel W, Forstmann BU (2016) A Neural Model of Mind Wandering. Trends Cogn Sci 20:570–578.

Mortaheb S, Van Calster L, Raimondo F, Klados MA, Boulakis PA, Georgoula K, Majerus S, Van De Ville D, Demertzi A (2022) Mind blanking is a distinct mental state linked to a recurrent brain profile of globally positive connectivity during ongoing mentation. Proc Natl Acad Sci U S A 119:e2200511119.

Philippi CL, Bruss J, Boes AD, Albazron FM, Deifelt Streese C, Ciaramelli E, Rudrauf D, Tranel D (2021) Lesion network mapping demonstrates that mind-wandering is associated with the default mode network. J Neurosci Res 99:361–373.

Qin P, Wang M, Northoff G (2020) Linking bodily, environmental and mental states in the self—A three-level model based on a meta-analysis. Neurosci Biobehav Rev 115:77–95.

Raeva SN (2006) The Role of the Parafascicular Complex (CM-Pf) of the Human Thalamus in the Neuronal Mechanisms of Selective Attention. Neurosci Behav Physiol 36:287–295.

Ramanan S, Piguet O, Irish M (2018) Rethinking the Role of the Angular Gyrus in Remembering the Past and Imagining the Future: The Contextual Integration Model. Neuroscientist 24:342–352.

Salvatier J, Wiecki TV, Fonnesbeck C (2016) Probabilistic programming in Python using PyMC3. PeerJ Comput. Sci. 2:e55.

Seeley WW, Menon V, Schatzberg AF, Keller J, Glover GH, Kenna H, Reiss AL, Greicius MD (2007) Dissociable Intrinsic Connectivity Networks for Salience Processing and Executive Control. Journal of Neuroscience 27:2349–2356 Publisher: Society for Neuroscience Section: Articles.

Seghier ML (2013) The angular gyrus: Multiple functions and multiple subdivisions. Neuroscientist 19:43–61.

Seli P, Risko EF, Smilek D, Schacter DL (2016) Mind-Wandering With and Without Intention. Trends Cogn Sci 20:605–617.

Smallwood J, Brown K, Baird B, Schooler JW (2012) Cooperation between the default mode network and the frontal-parietal network in the production of an internal train of thought. Brain Res 1428:60–70.

Smallwood J, Schooler JW (2015) The science of mind wandering: Empirically navigating the stream of consciousness. Annu Rev Psychol 66:487–518.

Smallwood J, Turnbull A, Wang Ht, Ho NSP, Poerio GL, Karapanagiotidis T, Konu D, Mckeown B, Zhang M, Murphy C, Vatansever D, Bzdok D, Konishi M, Leech R, Seli P, Schooler JW, Bernhardt B, Margulies DS, Jefferies E (2021) The neural correlates of ongoing conscious thought. iScience 24:102132.

Sormaz M, Murphy C, Wang Ht, Hymers M, Karapanagiotidis T, Poerio G, Margulies DS, Jefferies E, Smallwood J (2018) Default mode network can support the level of detail in experience during active task states. Proc Natl Acad Sci U S A 115:9318–9323.

Vaccaro AG, Fleming SM (2018) Thinking about thinking: A coordinate-based meta-analysis of neuroimaging studies of metacognitive judgements. Brain Neurosci Adv 2:2398212818810591.

Van Calster L, D'Argembeau A, Salmon E, Peters F, Majerus S (2017) Fluctuations of Attentional Networks and Default Mode Network during the Resting State Reflect Variations in Cognitive States: Evidence from a Novel Resting-state Experience Sampling Method. J Cogn Neurosci 29:95–113.

Vanhaudenhuyse A, Demertzi A, Schabus M, Noirhomme Q, Bredart S, Boly M, Phillips C, Soddu A, Luxen A, Moonen G, Laureys S (2011) Two distinct neuronal networks mediate the awareness of environment and of self. J Cogn Neurosci 23:570–578.

Vincent JL, Kahn I, Snyder AZ, Raichle ME, Buckner RL (2008) Evidence for a frontoparietal control system revealed by intrinsic functional connectivity. J Neurophysiol 100:3328–3342.

Ward A, Wegner D (2013) Mind-blanking: When the mind goes away. Front Psychol 4:650.

Weinstein Y (2018) Mind-wandering, how do I measure thee with probes? Let me count the ways. Behav Res 50:642–661.

Winter U, LeVan P, Borghardt TL, Akin B, Wittmann M, Leyens Y, Schmidt S (2020) Content-Free Awareness: EEG-fcMRI Correlates of Consciousness as Such in an Expert Meditator. Front Psychol 10:3064.

Wyland CL, Kelley WM, Macrae CN, Gordon HL, Heatherton TF (2003) Neural correlates of thought suppression. Neuropsychologia 41:1863–1867.

# Figures

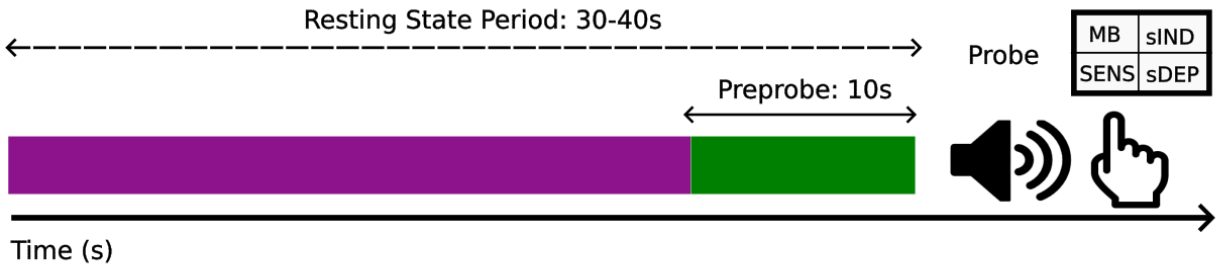


Figure 1: **Single trial of the experience-sampling paradigm**. During experience-sampling participants are asked to restfully lay in the scanner with eyes open and let their mind wander without any further orientation as to the focus of their thoughts. At random intervals (30-60 sec), participants are probed with an auditory cue to report the content of their thoughts at the moment preceding the probe using button press. Four available report categories were presented as available: Mind-Blanking (MB), Sensations (Sens), stimulus-independent thoughts (sIND), and stimulus-dependent thoughts (sDEP). For subsequent analysis, only the final 10 seconds of the resting period (green segment) were used.

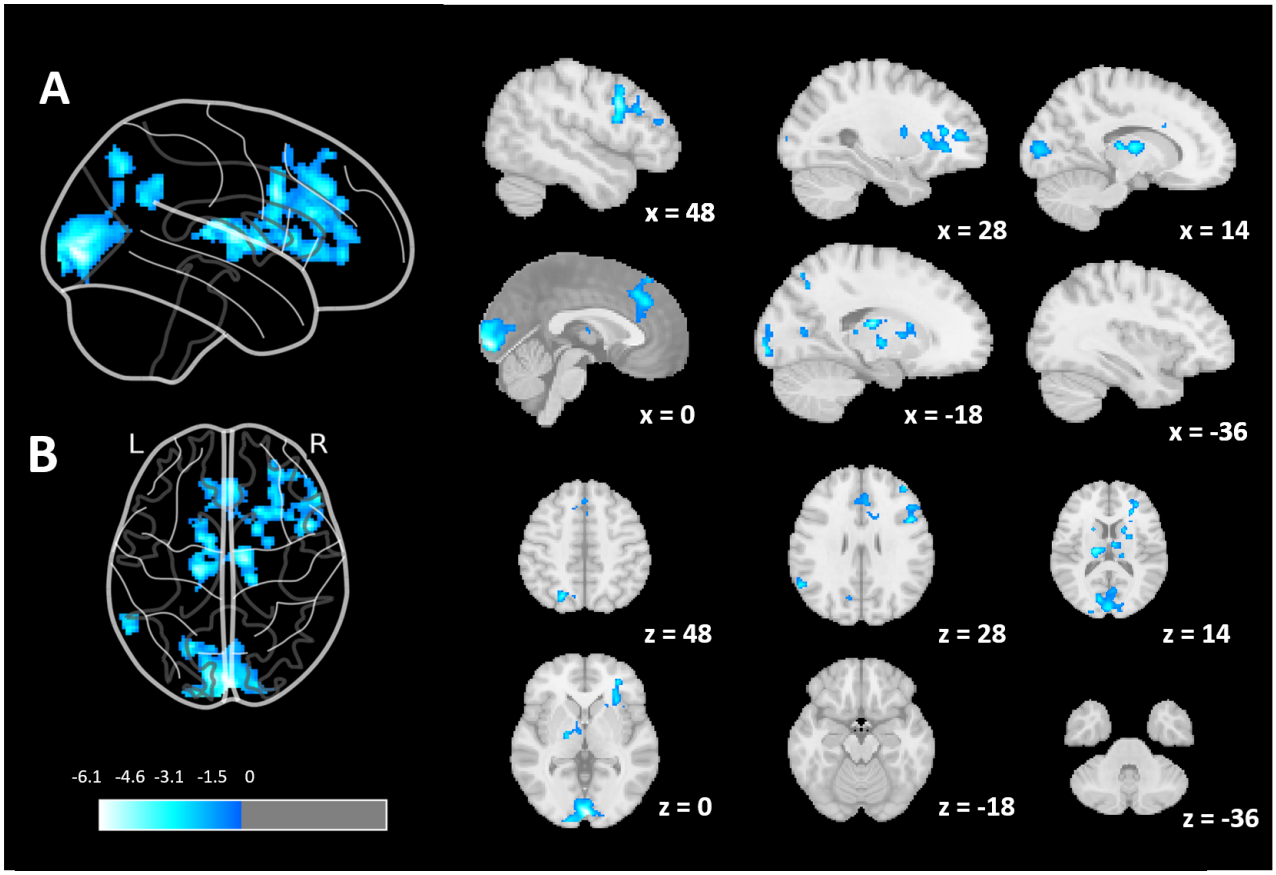


Figure 2: **fMRI univariate analysis of MB reports reveals whole-brain deactivations.** Statistically significant deactivations were observed in the anterior/midcingulate cortex, the calcarine cortex, the bilateral thalami, the right anterior insula, the precentral gyrus, and the left superior parietal lobule. A) Glass brain projection (sagittal and axial views) B) Activation map projected on the MNI152cortical template (sagittal and axial views). Color-bar indicates T-statistic. Maps are calculated on 10 seconds preceding MB reports. Results are identified at uncorrected voxel-level $p_{uncorrected} < 001$, and FDR-corrected at the cluster level $p_{FDR} < .05$.

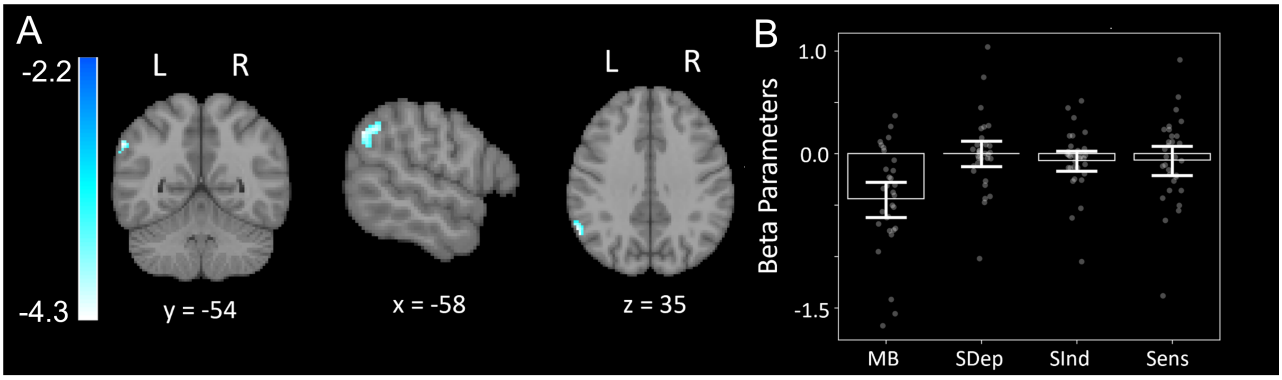


Figure 3: **fMRI contrast analysis between content-oriented reports and MB at a lower exploratory threshold reveals deactivations in the left angular gyrus.** (A) Significant clusters were identified at uncorrected voxel level $p_{uncorrected}<.001$ and a cluster threshold of 50 voxels. Color-bar indicates T-statistic. B) Boxplots representing the beta parameters of each individual state in the cluster of the left angular gyrus. Error bars indicate 95% confidence intervals. Datapoints show single-subject parameter values.

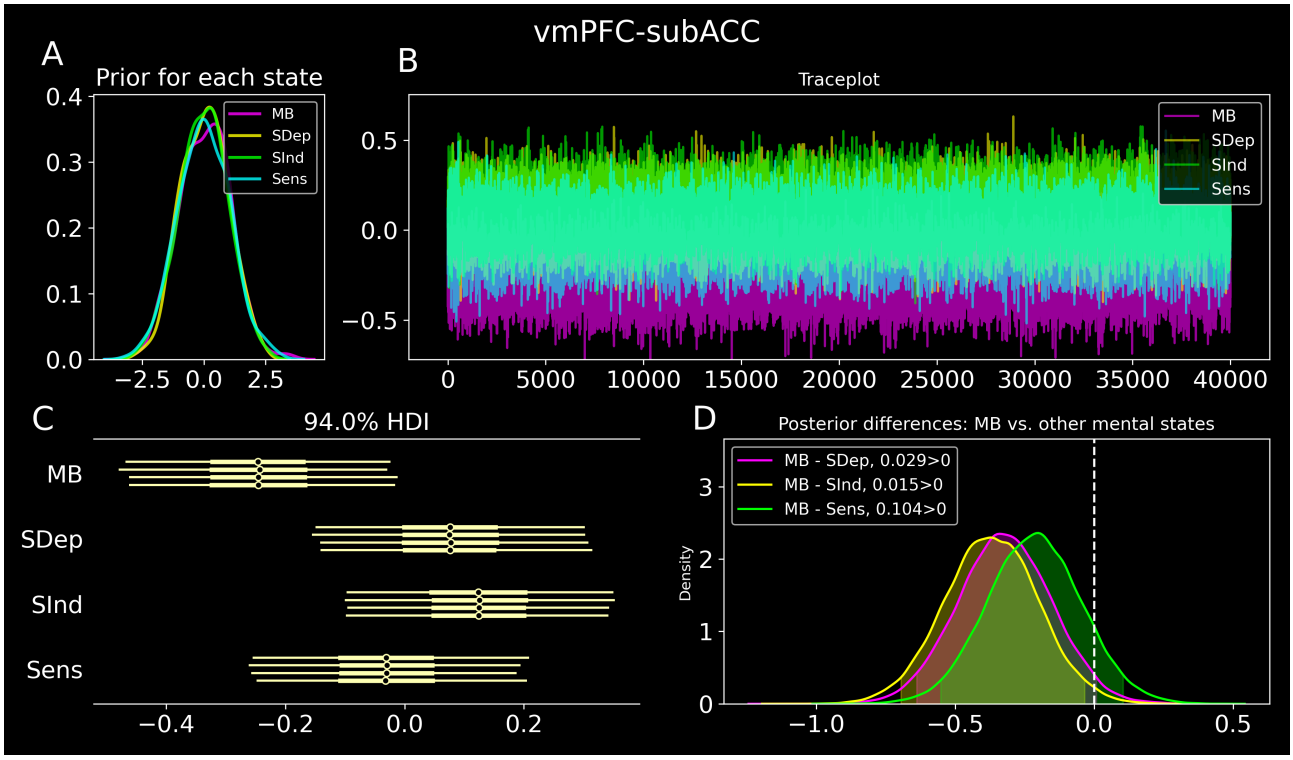


Figure 4: **Bayesian analysis of the beta parameters in the vmPFC/ACC ROI reveals deactivations in this area.** A) Null model prior expectations, modelling each prior as $N(0, 1)$. B) Traceplot of the model fit. Visual inspection of the random walk indicates that models converged, as the chains sampled the whole posterior space without autocorrelated data and sequential sampling of the same posterior space. C) Forest plot of each of the 4 sampled chains of the posterior distribution indicate that vmPFC/ACC contains evidence for contribution only MB, as it does not contain 0 in the HDI, showing model convergence. Each line represents 94% highest density intervals (HDI). During MB there was significant evidence for lower beta values as they did not include 0 in their 94% highest density intervals. This was not the case for the rest of the mental states. D) Posterior differences between MB and the rest of the mental states. We observed that the contrast MB-SInd did not contain 0 in the 94% HDI, providing evidence that frontal deactivations differentiate between MB and stimulus independent thoughts.

# Tables

Table 1: FMRI univariate analysis reveals deactivations during 5 TRs preceding MB reports.

| Region | No. of Voxels | Z | x | y | z |
|---|---|---|---|---|---|
| Right Calcarine Cortex | 1852 | 4.91 | 2 | -92 | 0 |
| Left Calcarine Cortex | | 4.67 | -8 | -88 | 6 |
| Left Occipital Pole | | 4.23 | -16 | -100 | -4 |
| Right Thalamus | 758 | 4.64 | 12 | -12 | 8 |
| Left Thalamus | | 4.61 | -18 | -18 | 16 |
| Right Precentral Gyrus | 1280 | 4.62 | 48 | 10 | 32 |
| Right Middle Frontal Gyrus | | 4.31 | 54 | 28 | 22 |
| Right Caudate | | 4.26 | 20 | 20 | 6 |
| Left Superior Parietal Lobule | 158 | 4.31 | -22 | -68 | 46 |
| Left Precuneus | | 3.19 | -12 | -68 | 46 |
| Superior Medio-Frontal Gyrus | 731 | 4.28 | 2 | 36 | 34 |
| Right Anterior/Midcingulate Cortex | | 3.90 | 6 | 32 | 22 |
| Right Anterior Insula | | 3.61 | 30 | 24 | 0 |
| Left Supramarginal Gyrus | 167 | 3.99 | -58 | -56 | 28 |

*Note*: An uncorrected voxel-level threshold of $p = 0.01$ was set and FDR-corrected at the cluster level $p < .05$. The X, Y, and Z coordinates refer to the AAL anatomical labeling map.

Table 2: Descriptive statistics for the posterior distributions of the beta parameters for each ROI and mental state.

| Region of Interest | Posterior | Median | SD | HDI (0.025) | HDI (0.975) |
|---|---|---|---|---|---|
| vmPFC-ACC | MB | -0.243 | 0.119 | -0.483 | -0.01 |
| | SDep | 0.0765 | 0.117 | -0.151 | 0.305 |
| | SInd | 0.124 | 0.119 | -0.098 | 0.369 |
| | Sens | -0.030 | 0.119 | -0.269 | 0.198 |
| | MB-All | -0.300 | 0.119 | -0.539 | -0.066 |
| | MB-SDep | -0.319 | 0.167 | -0.651 | 0.004 |
| | MB-SInd | -0.367 | 0.168 | -0.690 | -0.028 |
| | MB-Sens | -0.213 | 0.169 | -0.548 | 0.116 |
| Broca's Area | MB | -0.062 | 0.063 | -0.194 | 0.056 |
| | SDep | -0.072 | 0.065 | -0.201 | 0.055 |
| | SInd | -0.11 | 0.064 | -0.239 | 0.011 |
| | Sens | -0.183 | 0.064 | -0.310 | -0.060 |
| | MB-All | 0.061 | 0.063 | -0.070 | 0.180 |
| | MB-SDep | 0.009 | 0.091 | -0.170 | 0.184 |
| | MB-SInd | 0.049 | 0.090 | -0.127 | 0.232 |
| | MB-Sens | 0.123 | 0.091 | -0.053 | 0.301 |
| Left Hippocampus | MB | 0.024 | 0.072 | 0.119 | 0.166 |
| | SDep | 0.117 | 0.072 | -0.026 | 0.254 |
| | SInd | 0.113 | 0.072 | -0.033 | 0.250 |
| | Sens | 0.028 | 0.073 | -0.117 | 0.166 |
| | MB-All | -0.063 | 0.073 | -0.205 | 0.082 |
| | MB-SDep | -0.094 | 0.103 | -0.304 | 0.102 |
| | MB-SInd | -0.090 | 0.102 | -0.289 | 0.108 |
| | MB-Sens | -0.005 | 0.103 | -0.201 | 0.202 |

*Note*: HDI: highest density interval.

Table 3: Model comparison of fitted models.

| Region of Interest | Model | WAIC | ELPD |
|---|---|---|---|
| vmPFC-ACC | Fitted | -130.438 | -130.653 |
| | Null | -130.790 | -130.891 |
| Broca's Area | Fitted | -51.271 | -51.292 |
| | Null | -49.505 | -49.512 |
| Left Hippocampus | Fitted | -62.479 | -62.557 |
| | Null | -60.249 | -60.285 |

*Note*: WAIC = Watanabe–Akaike information criterion, ELPD = Expected log pointwise predictive density.